

Infrared photoelectron tunneling spectroscopy of strongly coupled quantum wells

K. K. Choi

U.S. Army Electronics Technology and Devices Laboratory, Fort Monmouth, New Jersey 07703-5000

B. F. Levine, C. G. Bethea, J. Walker, and R. J. Malik

AT&T Bell Laboratories, Murray Hill, New Jersey 07974

(Received 21 November 1988)

Infrared photoelectron tunneling spectra have been obtained for two different strongly coupled quantum-well structures. With this new spectroscopic technique, the energy-level structure and the internal-field configuration of the quantum-well structures at different biases can be determined accurately. The results agree with the numerical calculations performed for these structures. The observation of multiple peaks in the photoresponse in these devices indicates the possibility of multicolor infrared detection.

Recent observations of infrared intersubband absorption^{1,2} in GaAs/Al_xGa_{1-x}As multiple quantum wells provide a new technique to determine the energy levels confined by the conduction-band discontinuity. One advantage of this technique is that it provides more direct information about the energy states in the conduction band than the conventional photoluminescence³ and electroluminescence^{4,5} techniques, since the new technique does not involve the band structures of the holes. However, the intersubband absorption signal can be masked by other extrinsic processes, such as plasmon absorption in the contact layers, optical-phonon absorption in the substrate layer, and Fabry-Pérot oscillations between the epilayers. In the following we introduce a new kind of spectroscopy, infrared photoelectron tunneling (IPET) spectroscopy, for which the observed signal is sensitive specifically to the intersubband absorption and hence is more reliable. We apply this technique to two different strongly coupled quantum-well structures and obtain detailed information about the energy levels in the presence of an applied electric field. We also solve numerically the Schrödinger equation for the structures using the transfer-matrix technique⁶ in order to analyze quantitatively the experimental results.

The first sample under study was grown with 50 periods of 65-Å GaAs quantum well (doped at $n=1.0\times 10^{18}$ cm⁻³), 40-Å undoped Al_{0.25}Ga_{0.75}As, 14-Å undoped GaAs, and 150-Å undoped Al_{0.25}Ga_{0.75}As. The quantum wells are sandwiched between the top (0.5 μm) and the bottom (1 μm) GaAs contact layers in which $n=1\times 10^{18}$ cm⁻³. The band diagram of a single period under bias is shown in the inset of Fig. 1. If the wells were isolated, there would be two bound levels ($E_1=50$ meV, $E_2=181$ meV) in the 65-Å well and one level ($E'_1=163$ meV) in the 14-Å well. In the actual structure E_2 and E'_1 are coupled, thus shifting the energy levels to the values $E_1=50$ meV, $E_2=154$ meV, and $E_3=188$ meV. The resulting wave functions for these bound states, together with that for the first continuum state (ψ_4) are depicted in Fig. 2. (Using the coupled-energy scheme, we have adjusted the quoted well widths slightly from the nominal values to match the infrared absorption peaks shown in Fig. 1.)

Based on these wave functions, the oscillator strength (f_n) between the ground state and the excited state n can be calculated, and the results are $f_2=0.46$, $f_3=0.45$, and $f_4=0.13$.⁷ The approximate equality between f_2 and f_3 is consistent with the equal absorption amplitudes at ν_2^0 and ν_3^0 shown in Fig. 1, where ν_n^0 denotes the fitted wave number of the absorption peak due to the transition between the ground state and the n th state at zero bias. The expected weaker absorption at ν_4^0 is not observable in the absorption curve due to the rapidly rising background on both sides. Strikingly, this optical transition can be observed unambiguously in the IPET spectroscopy introduced here.

In order to obtain the IPET spectrum, devices suitable for photoresponse measurements are fabricated on a substrate with a 45° angle at the edge. At a temperature $T=15$ K, continuous tunable infrared radiation obtained from a chopped (4 kHz) glow-bar source and a monochromator is incident normal to the substrate edge.^{8,9} The photocurrent generated (I_p) is monitored by a 100-kΩ series resistor at different biases.

Figure 1 shows the IPET spectra at two biasing conditions. The solid curve shows the spectrum when the device is under reverse bias with the potential drop per period $V_p=63.5$ mV, whereas the dashed curve shows the spectrum under forward bias with a similar V_p (58.4 mV). Under reverse bias, three peaks in the spectrum are observed, in contrast with the forward-biasing case where only one peak with a left shoulder is found. In order to understand the origin of these peaks, we solve numerically the Schrödinger equation for forward and reverse biases, assuming a linear potential drop within the structure. The resulting transition energies are indicated by the inverted triangles in Fig. 1. They are generally very close to the observed peaks, allowing the assignment of the peaks. For example, under reverse bias the peaks at $\nu=970$, 1190, and 1300 cm⁻¹ can be attributed to the transitions from the ground state to the second, third, and fourth excited states, respectively. In order to match the spectra more precisely, we adjust the potential drop between the center of the wells (V_c) from $0.3V_p$ (assuming a linear potential drop) to $0.45V_p$ in both biases. With the new potential

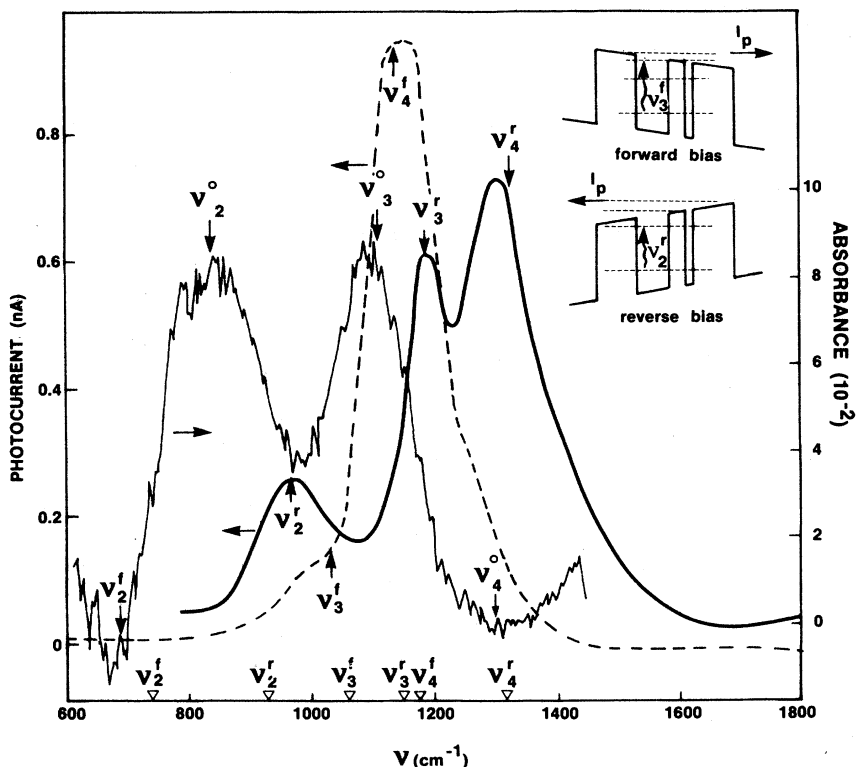


FIG. 1. The infrared absorption spectrum (for sample having the waveguide geometry) and the IPET spectra for forward bias (dashed curve) and reverse bias (solid curve). The inverted triangles indicate the transition energies assuming linear potential drop. The arrows indicate fitted transition energies with different V_c . The insets indicate the device under different biasing conditions.

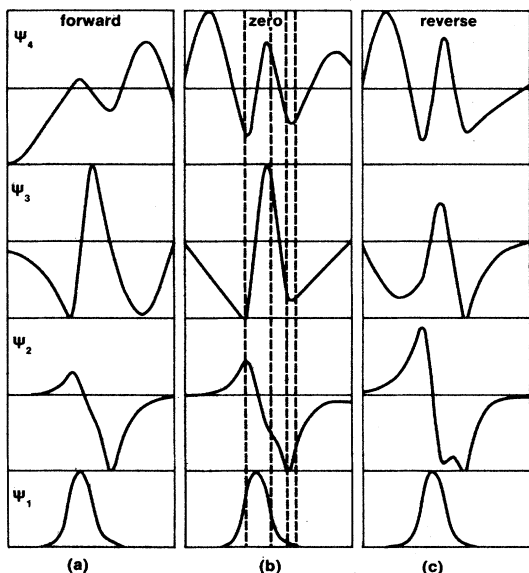


FIG. 2. The shape of the wave functions in the coupled quantum-well structure under (a) forward, (b) zero, and (c) reverse biases. The theoretical oscillator strength under bias is based on the shape of these wave functions. The dashed lines indicate the locations of the band-edge discontinuity.

configuration all the peaked structures can be matched simultaneously, as shown by the arrows in Fig. 1, indicating the consistency of the theoretical interpretation and the experiment. The nonlinearity of the potential drop might be expected due to the screening of the electrons in the doped well and the non-Ohmic nature of the tunneling barriers. These shifts of the peak positions show that the wells are strongly coupled. For example, if the wells were isolated the maximum upward shift of ν_3^f could only be 16 cm^{-1} (Stark shift) by assuming all the potential drop within the thicker well, contrary to the experimental shift (100 cm^{-1}).

In order to understand the general shape of the spectrum, let us recall that the photocurrent is approximately proportional to the number of the electrons excited per unit time, the tunneling probability p , and the hot-electron mean free path.^{10,11} While the former depends on the oscillator strength, the latter two are proportional to the energy of the excited state, and thus tend to cause I_p to increase with the excitation energy, qualitatively consistent with the experiment. In particular, the resonant state E_4 , which is undetected in the absorption spectrum, is greatly enhanced compared with the bound states. On the other hand, the I_p from the second level under forward bias is suppressed due to the small transmission coefficient out of the well. The asymmetry observed between the two biases

is due to the fact that under forward bias, the level E_1' moves toward E_1 , and hence the transition energies are reduced, while under reverse bias the opposite is true and the transition energies are increased.

In order to do a more-quantitative analysis, we have estimated the relevant quantities. In particular, under reverse bias the oscillator strengths are found to be $f_2=0.76$, $f_3=0.11$, and $f_4=0.14$. The fact that $f_2 \gg f_3$ under this bias greatly compensates the difference in the tunneling probabilities ($p_2=0.31$ and $p_3=0.91$) and leads to comparable I_p . Combining these factors with the mean free paths, we estimate the ratio of I_p at ν_2^f , ν_3^f , and ν_4^f to be 1.8:1:1.3. The ratio between ν_3^f and ν_4^f is consistent with this observation. However, due to the small tunneling probability p_2 that is sensitively dependent on the quantum well parameters, we overestimate I_p at ν_2^f by a factor of 2. A more-elaborate calculation will give more precise results.^{12,13} However, such an exercise is not the focus of this work.

Next, we describe the infrared absorption and the IPET spectra of another device structure that shows additional characteristics. The photoresponse of this device at a single radiation energy was reported previously.¹³ The device consists of 50 periods of 72-Å GaAs (doped at $n=1 \times 10^{18} \text{ cm}^{-3}$), 39-Å undoped $\text{Al}_{0.31}\text{Ga}_{0.69}\text{As}$, 20-Å undoped GaAs, and 154-Å undoped $\text{Al}_{0.31}\text{Ga}_{0.69}\text{As}$.¹⁴ The barrier height of this device is higher than the former device, and hence the coupling between the wells is weaker. The calculated transition energies for this structure, ν_2^0 , ν_3^0 , and ν_4^0 (indicated in Fig. 3), are in satisfactory agreement with the absorption spectrum except for the absence of the ν_2^0 peak. A calculation of the oscillator strengths [$f_2=0.27$, $f_3=0.75$, and $f_4=0.01$ (Ref. 7)] shows that the apparent absorption strengths at ν_2^0 and ν_4^0 could have been modified by the background absorption due to the small oscillator strengths. The IPET spectrum, however, is quite clearly showing three I_p peaks under reverse bias, indicating that three optical transitions must be occurring in this energy range, despite only two absorption peaks being observed.

The IPET spectra of this device again show all the expected features. The spectra are obtained at significantly higher biases than that for the previous device (due to the higher barriers), namely a forward bias of $V_p=109 \text{ mV}$ (dashed curve) and a reverse bias of $V_p=123 \text{ mV}$ (solid curve). The peaks can be fitted with V_c being equal to $0.3V_p$ (i.e., linear potential drop), but are slightly better fitted with $V_c=0.45V_p$ for the forward bias and $V_c=0.25V_p$ for the reverse bias as shown in Fig. 3. At these large biases, the effect of the electron screening is increased due to the increasing distortion of the wave function. Since the ground-state wave function is primarily located in the thicker well, there is an asymmetry in the screening under different biasing polarity at large biases. That is, the slightly larger V_c under forward bias can be attributed to the lack of electron screening in the thin well.

As already noted above, the ν_2^f peak (although absent in the absorption spectrum) is evident in the IPET spectrum. This observation is due to the enhanced f_2 ($f_2=0.74$, $f_3=0.26$) under reverse bias. Another striking feature in

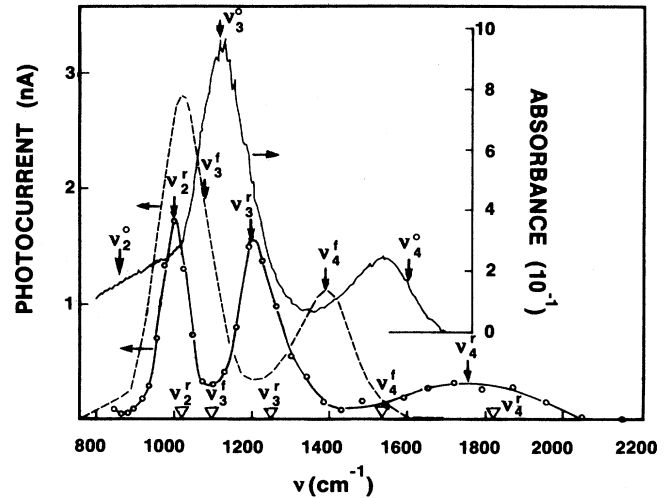


FIG. 3. The infrared absorption spectrum and the IPET spectra for forward bias (dashed curve) and reverse bias (solid curve joining the circles). The circles are the experimental data points showing the typical scattering of the data. The triangles indicate the transition energies assuming linear potential drop. The arrows indicate fitted transition energies with different V_c . ν_2^f ($=548 \text{ cm}^{-1}$) is out of the scale and is not shown.

this spectrum is the broad I_p peak associated with ν_4^f observed around 1800 cm^{-1} . It indicates that although this level is significantly above the barriers (40 meV above), the level is still relatively well defined, confirming the existence of the Stark ladder even for the extended continuum states, as found in the tunneling characteristics reported previously.^{11,13}

The large f_3 under forward bias ($f_2=0.19$, $f_3=0.85$) contributes to the large I_p near ν_3^f . The fact that the photocurrent peak near ν_3^f does not coincide with the calculated absorption peak is a noteworthy feature of the IPET spectroscopy. Since I_p is proportional to both the absorption strength and the tunneling probability at a particular energy, I_p is peaked at the maximum absorption only if p is a monotonic function of energy. For the present device, it is designed such that p is peaked (close to unity) near $\nu=1000 \text{ cm}^{-1}$ using the coherent tunneling mechanism;¹³ the resulting I_p is peaked toward the energy where p is a maximum and the combined factors make this peak dominant over all the other peaks. We emphasize that based on the observed absorption peak ν_3^0 at zero bias, one cannot adjust any values of V_c or the width of the thin well such that ν_3^f coincides with the photocurrent peak. This is because when eV_c is large, the energy separation between the levels E_2 and E_1' of the individual wells becomes larger than the tunneling lifetime of the levels. In this case the levels will be decoupled and the transition energy ν_3^f becomes insensitive to either V_c (as indicated by the calculated values for $V_c=0.3V_p$ and $0.45V_p$ shown in Fig. 3) or the energy level associated with the thin well.

In conclusion, we have introduced a new spectroscopy in which the photocurrent is continually monitored with a

tunable infrared radiation source. Applying this technique to the coupled quantum-well structures, we can determine accurate information about the level structure of the quantum wells, the oscillator strengths, and their internal field configurations, which are not readily obtainable by other means. Our calculations demonstrate that

IPET spectroscopy can be more sensitive (at large bias) and more reliable than absorption spectroscopy. In these devices which have unequal quantum-well thickness, the parity symmetry is broken, leading to nonzero oscillator strengths between the levels. Based on this unique property, a multicolor infrared photodetector may be possible.

-
- ¹L. C. West and S. J. Eglash, *Appl. Phys. Lett.* **46**, 1156 (1985).
²B. F. Levine, R. J. Malik, J. Walker, K. K. Choi, C. G. Bethea, D. A. Kleinman, and J. M. Vandenberg, *Appl. Phys. Lett.* **50**, 273 (1987).
³R. C. Millar, D. A. Kleinman, and A. C. Gossard, *Phys. Rev. B* **29**, 7085 (1984).
⁴H. Q. Le, J. J. Zayhowski, W. D. Goodhue, and J. Bales, in *Proceedings of the Thirteenth International Symposium on GaAs and Related Compounds, Las Vegas, Nevada, 1986*, edited by W. T. Lindley (Institute of Physics, Bristol, 1986), p. 319; *Appl. Phys. Lett.* **50**, 1518 (1987).
⁵A. Kastalsky, T. Duffield, S. J. Allen, and J. Harbison, *Appl. Phys. Lett.* **52**, 1320 (1988).
⁶B. Ricco and M. Ya Azbel, *Phys. Rev. B* **29**, 1970 (1984).
⁷Since the fourth state is a resonant state, its wave function is slowly varying with time. The indicated wave function and the derived f_4 are approximations.
⁸B. F. Levine, C. G. Bethea, K. K. Choi, J. Walker, and R. J. Malik, *Appl. Phys. Lett.* **53**, 231 (1988).
⁹B. F. Levine, C. G. Bethea, G. Hasnain, J. Walker, and R. J. Malik, *Appl. Phys. Lett.* **53**, 296 (1988).
¹⁰B. F. Levine, K. K. Choi, C. G. Bethea, J. Walker, and R. J. Malik, *Appl. Phys. Lett.* **50**, 1092 (1987).
¹¹K. K. Choi, B. F. Levine, C. G. Bethea, J. Walker, and R. J. Malik, *Appl. Phys. Lett.* **50**, 1814 (1987).
¹²B. F. Levine, K. K. Choi, C. G. Bethea, J. Walker, and R. J. Malik, *Appl. Phys. Lett.* **51**, 934 (1987).
¹³K. K. Choi, B. F. Levine, C. G. Bethea, J. Walker, and R. J. Malik, *Phys. Rev. Lett.* **59**, 2459 (1987).
¹⁴In this work, we found the Al molar ratio $x=0.31$ and the thin well width $W=20$ Å fit the entire spectrum slightly better than $x=0.33$ and $W=18$ Å originally adopted in Ref. 11. $W=18$ Å fits the spectrum with smaller $V_c (=0.15V_p)$ under reverse bias. The conclusions in both papers are not affected.